NEOShield-2

Science and Technology for Near-Earth Object Impact Prevention

Grant agreement no:	640351	Project Start:	1 March 2015
Project Coordinator	Airbus Defence and Space DE	Project Duration:	31 Months

WP 10.2 Deliverable D10.4	**Report on Photometric Observations I (Colours, and Phase Functions)**		
WP Leader	OBSPM	Task Leader	INAF
Due date	M29, 31 Jul 2017		
Delivery date	21.07.2017		
Issue	1.1 (FINAL)		
Editor (authors)	S. Ieva, E. Dotto, E. Mazzotta Epifani, A. Di Paola, R. Speziali, M. Lazzarin, I. Bertini, A. Giunta		
Contributors	D. Lazzaro, P. Arcoverde, V. Petropoulou, P. Ochner		
Verified by			
Document Type	R		
Dissemination Level	PU		

The NEOShield-2 Consortium consists of:		
Airbus Defence and Space GmbH (Project Coordinator)	ADS-DE	Germany
Deutsches Zentrum für Luft- und Raumfahrt e.V.	DLR	Germany
Airbus Defence and Space SAS	ADS-FR	France
Airbus Defence and Space Ltd	ADS-UK	United Kingdom
Centre National de la Recherche Scientifique	CNRS	France
DEIMOS Space Sociedad Limitada Unipersonal	DMS	Spain
Fraunhofer-Gesellschaft zur Förderung der angewandten Forschung e.V.	EMI	Germany
GMV Aerospace and Defence SA Unipersonal	GMV	Spain
Istituto Nazionale di Astrofisica	INAF	Italy
Observatoire de Paris	OBSPM	France
The Queen's University of Belfast	QUB	United Kingdom

This project has received funding from the European Union's Horizon 2020 research and innovation programme under grant agreement No 640351.

Change Record

Issue	Date	Section, Page	Description of Change
1.0	07/07/2017		First Draft. Distributed to Consortium.
1.1	21/07/2017		FINAL version. Incorporating comments from Consortium.

Table of Contents

1 Introduction

1.1 Scope

In the framework of the WP10, INAF was the leader of the Task 10.2.1 "Colours and Phase Functions". In order to obtain B-V-R-I photometric measurements for a large sample of NEOs and determine their colour indexes and their taxonomic classification we submitted a competitive proposal to TNG. We were awarded with 96h, splitted in 6 runs of 4 hours each and going on for 4 semesters (September 2015 – September 2017). We were also awarded with observational time (4h) at LBT to characterize, in the B-V-R-I-g-r-z filters, fainter objects that were not observable from TNG (V > 21), in order to debias our sample towards fainter NEOs. Finally, we made use of the Italian Asiago Schmidt telescope to characterize NEO B-V-R-I colour indexes. We obtained colour indexes for 231 uncharacterized NEOs, although some of them show a low S/N in one or more filters, and were therefore excluded to the subsequent analysis.

Since September 2015 we established an agreement with Daniela Lazzaro to use the 1m OASI telescope in Brazil, in order to perform the phase curve characterization of several interesting NEOs each month. To the same use, starting from May 2016, we made use of the Italian Campo Imperatore 1m telescope. Although some technical problems and some inconvenient weather conditions, we were able to characterize several NEO phase curves, greatly incrementing the number of NEO phase curves available in literature.

1.2 List of Abbreviations

AD	Applicable Document
AU	Astronomical Unit
CCD	Charge-Coupled Device
DoA	Description of Action
GA	Grant Agreement
INAF	Istituto Nazionale di Astrofisica
LBT	Large Binocular Telescope
LTP	Long Term Programme
MOID	Minimum Orbit Intersection Distance
NEA	Near Earth Asteroid
NEO	Near Earth Object
OASI	Observatorio Astronomico do Sertao do Itaparica
RD	Reference Document
RMS	Root-Mean-Square
TNG	Telescopio Nazionale Galileo
WP	Work Package

1.3 Applicable Documents

[AD1] NEOShield-2: "Science and Technology for Near-Earth Object Impact Prevention", Grant Agreement no. 640351, 28.10.2014.

1.4 Reference Documents

[RD1] Popescu, M., Birlan, M., Nedelcu, D. A. (2012). Modeling of asteroid spectra - M4AST. A&A, 544, A130

[RD2] DeMeo, F. E., Binzel, R.P., Silvan, S. M. and Bus, S. J. (2009). An extension of the Bus asteroid taxonomy into the near-infrared. Icarus, 202, 160.

[RD3] Perna, D., Dotto, E., Ieva, S., et al. (2016). Grasping the Nature of Potentially Hazardous Asteroids. AJ, 151, 11

[RD4] Holsapple K. A. (2004), in Mitigation of hazardous comets and asteroids, University Press, Cambridge, UK

[RD5] Perna, D., Barucci, M. A., Fulchignoni, M. (2013). The near-Earth objects and their potential threat to our planet. A&ARv, 21, 65

[RD6] Hicks, M. D.; Bambery, R. J.; Lawrence, K. J. et al. (2007). Near-nucleus photometry of comets using archived NEAT data. Icarus, 188, 457

[RD7] Hicks, M. & Thackeray, B. (2016). Spin Rate of Comet 333P/LINEAR (2007 VA85). ATel, 8905

[RD8] Penttilä, A.; Shevchenko, V. G.; Wilkman, O. et al. (2016). H, G_1, G_2 photometric phase function extended to low-accuracy data. P&SS, 123, 117

2 WP 10.2.1 "Colours and Phase Functions".

Our team was responsible of the work package 10.2.1. "Colours and Phase functions", which has the aim to acquire photometric measurements in order:

- to perform a taxonomic classification using computed color indexes and have the first constraints on the surface composition and albedo of the observed objects;
- to study the phase function, and to derive NEO β and G parameters to better compute the absolute magnitude. The obtained phase functions will also give an independent confirmation of the taxonomic classification;
- to combine the results obtained in the visible bands with thermal infrared observations, already planned in the framework of the NEOShield-2 project, to obtain information on the surface physical properties (e.g. regolith, thermal inertia);
- to derive a rough estimation of the internal density from the taxonomic classification computed using color indexes and phase function, in order to estimate the response to non-gravitational forces (mainly to the Yarkovsky effect), therefore modelling their future dynamical evolution.

To this purpose, we had access to Italian telescopes and facilities (e.g. Campo Imperatore, Asiago), as well as we submitted observational proposals to have access to medium/large and very large telescopes (e.g. TNG, LBT). We also established an agreement with the OASI-Itacuruba telescope in Brazil to obtain phase curve characterization for several NEOs each month.

2.1 Colour indexes

Taxonomic classification of NEOs based upon photometric observations is a powerful tool to investigate the surface composition of a large sample of NEOs with a limited amount of observing time. With the coverage of BVRI photometry it is possible to compute colour indexes (B-V, V-R and V-I), hence have the first constraints on the taxonomical type, which give information on the surface composition and the albedo of the observed objects.
In order to derive a reliable taxonomy for each object we made use of an online classification algorithm, M4AST (Popescu et al. 2012 [RD1]) that adopts standard curve matching techniques to determine to which extent the reflectance of an asteroid is similar to a sample spectrum, one for each class portrayed in the DeMeo et al. (2009 [RD2]) taxonomy.

2.1.1 Observations at TNG

In September 2015 we were awarded with a LTP at TNG to perform photometric observations of B-V-R-I magnitudes for a large sample of NEOs. We requested and obtained 6 slots of 4h each semester, spanning four semesters, up to September 2017. At the moment 21 out of 24 runs were already executed (See Tab. 3-1). Five runs could not have been performed due to bad weather conditions. In the remaining 16 observing runs we obtained photometric observations for 188 NEOs.

30 targets are at the moment under reduction. For the remaining 158 targets data have been reduced and calibrated, and colour indexes and a preliminary taxonomy, when available, is shown in Tab. 3-2. Few targets show a low S/N in some, or every filter, and it was not possible to derive a reliable taxonomic classification. Therefore, they were excluded from the subsequent analysis.

Table 3-1: For each run of the LTP, we reported the allocated time, the number of successfully observed targets and comments.

Semester	Run	Allocated time	Observed Targets
AOT32	13th October 2015	4h	7 targets – data reduced and analyzed
AOT32	14th November 2015	4h	**No observations, bad weather**
AOT32	2nd December 2015	4h	13 targets – data reduced and analyzed
AOT32	10th December 2015	4h	15 targets – data reduced and analyzed
AOT32	8th January 2016	4h	**No observations, bad weather**
AOT32	11th February 2016	4h	15 targets – data reduced and analyzed
AOT33	6th April 2016	4h	15 targets – data reduced and analyzed
AOT33	2nd May 2016	4h	14 targets – data reduced and analyzed
AOT33	3rd June 2016	4h	12 targets – data reduced and analyzed
AOT33	2nd July 2016	4h	14 targets – data reduced and analyzed
AOT33	30th July 2016	4h	8 targets – data reduced and analyzed
AOT33	2nd September 2016	4h	11 targets – data reduced and analyzed
AOT34	30th September 2016	4h	12 targets – data reduced and analyzed
AOT34	22nd October 2016	4h	9 targets – data reduced and analyzed
AOT34	21st November 2016	4h	**No observations, bad weather**
AOT34	22nd December 2016	4h	**No observations, bad weather**
AOT34	20th January 2017	4h	**No observations, bad weather**
AOT34	27th February2017	4h	13 targets – data reduced and analyzed
AOT35	1st May 2017	4h	*7 targets – data under reduction*
AOT35	27th May 2017	8h	*23 targets – data under reduction*
AOT35	24th July 2017	8h	---
AOT35	21st September 2017	4h	---

Table 3-2: Observational date, colour indexes and taxonomy derived for the whole sample of targets characterized at TNG.

Object Name		Observational date	V	B-V	V-R	V-I	Taxonomy
423709	2006 BQ6	13/10/2015	21.63	0.65	0.57	1.28	NOISY
445974	2013 BJ18	13/10/2015	21.72	0.92	0.56	0.77	S
451370	2011 AK5	13/10/2015	19.42	1.16	0.35	0.73	X/C
	2006 BE55	13/10/2015	20.86	1.01	0.29	1.00	S
65690	1991 DG	13/10/2015	20.37	0.64	0.42	0.57	C
482796	2013 QJ10	13/10/2015	20.19	0.95	0.12	0.73	S
	2012 VO7	02/12/2015	19.98	0.57	***	0.72	NOISY
334673	2003 AL18	02/12/2015	19.89	0.79	0.48	***	C

Object Name		Observational date	V	B-V	V-R	V-I	Taxonomy
	2015 KJ57	02/12/2015	19.90	0.70	0.79	***	NOISY
96631	1999 FP59	02/12/2015	20.06	0.40	0.64	***	NOISY
	2015 OS35	02/12/2015	19.47	0.82	0.28	***	C
452397	2002 PD130	02/12/2015	20.31	0.85	0.54	***	S
144411	2004 EW9	02/12/2015	20.05	0.80	***	0.57	NOISY
459046	2012 AS10	02/12/2015	20.43	1.04	0.56	0.91	S
153271	2001 CL42	02/12/2015	20.19	0.88	0.21	***	NOISY
	2013 UG5	10/12/2015	20.09	0.59	0.42	0.65	C
	2015 RT83	10/12/2015	19.30	1.04	0.39	0.65	S
155110	2005 TB	10/12/2015	19.10	0.77	0.31	0.74	C
138852	2000 WN10	10/12/2015	19.57	1.13	0.27	0.63	X/S
442243	2011 MD11	10/12/2015	19.98	0.85	0.62	0.81	S
	2012 XA133	10/12/2015	19.82	0.89	0.39	0.47	S
142563	2002 TR69	10/12/2015	19.88	1.02	0.43	0.51	S
162273	1999 VL12	10/12/2015	19.51	0.86	0.55	0.84	V
453309	2008 VQ4	10/12/2015	19.78	0.94	0.33	0.69	C
443880	2001 UZ16	10/12/2015	20.20	0.57	0.44	0.61	C
	2011 YH6	10/12/2015	20.03	0.73	0.52	0.91	D
174806	2003 XL	10/12/2015	19.96	0.76	0.45	0.95	X
455199	2000 YK4	10/12/2015	20.45	0.81	0.41	0.89	S
194126	2001 SG276	10/12/2015	20.03	0.75	0.55	0.87	S
468005	2012 XD112	10/12/2015	19.78	0.99	0.50	0.69	S
430804	2005 AD13	11/02/2016	20.26	0.51	0.29	0.69	D
	2012 CK2	11/02/2016	19.61	0.70	0.38	0.59	C
	2016 AF165	11/02/2016	19.30	0.67	0.33	0.67	C
	2007 EA26	11/02/2016	19.81	0.62	0.30	0.77	S
403247	2008 XO2	11/02/2016	19.78	0.76	0.51	0.92	S
458375	2010 WY8	11/02/2016	19.84	1.15	0.10	0.37	NOISY
	2015 OL35	11/02/2016	19.40	0.77	0.52	0.75	S
	2016 AZ8	11/02/2016	20.01	0.37	0.51	0.57	NOISY
	2015 YN1	11/02/2016	20.01	0.68	0.59	0.85	S
6050	Miwablock	11/02/2016	20.44	0.74	0.40	0.74	C/X
4596	1981 QB	11/02/2016	21.13	1.05	0.47	0.96	S
453729	2011 BO24	11/02/2016	20.21	0.84	0.42	0.78	S/X

Object Name		Observational date	V	B-V	V-R	V-I	Taxonomy
458723	2011 KQ12	11/02/2016	19.49	1.24	0.50	0.68	V
	2012 BF86	11/02/2016	19.87	1.03	0.43	0.59	S
386504	2009 BP58	11/02/2016	20.01	1.07	0.33	0.49	S
250706	2005 RR6	06/04/2016	19.46	0.83	0.48	0.82	S
403247	2008 XO2	06/04/2016	19.75	0.93	0.53	0.48	S
466508	2014 GY48	06/04/2016	20.08	0.73	0.57	0.79	X
	2009 DL46	06/04/2016	20.07	0.65	0.47	0.89	D
334412	2002 EZ2	06/04/2016	18.95	0.73	0.44	0.79	X
	2015 WH9	06/04/2016	19.63	0.72	0.31	0.63	C
463360	2012 TU	06/04/2016	20.50	1.39	0.28	0.48	NOISY
458375	2010 WY8	06/04/2016	20.12	0.75	0.53	0.67	S
267136	2000 EF104	06/04/2016	18.98	0.83	0.46	0.72	S
	2006 HV5	06/04/2016	19.00	0.99	0.80	0.83	D
356285	2010 DE	06/04/2016	19.69	0.67	0.58	0.80	S
465824	2010 FR	06/04/2016	20.30	0.35	0.36	0.53	C
463282	2012 HR15	06/04/2016	19.82	0.72	0.49	0.82	X
	2016 FL12	06/04/2016	19.63	0.69	***	0.88	X
453729	2011 BO24	06/04/2016	19.79	0.61	0.45	0.62	S/C
411201	2010 LJ14	02/05/2016	19.54	0.91	0.56	0.74	V
447221	2005 UO5	02/05/2016	20.31	0.79	0.54	0.90	S
	2015 TX143	02/05/2016	19.58	0.77	0.52	0.72	S
	2016 EM28	02/05/2016	21.00	0.72	0.37	0.78	X
276392	2002 XH4	02/05/2016	20.21	0.68	0.46	***	X
468541	2006 QA31	02/05/2016	19.45	0.86	0.39	0.58	C
5370	Taranis	02/05/2016	20.10	0.64	0.36	0.82	C
	2009 DL46	02/05/2016	19.26	0.64	0.31	0.93	D
334412	2002 EZ2	02/05/2016	20.57	0.85	0.50	0.57	S
6050	Miwablock	02/05/2016	20.11	1.02	0.41	0.93	S
	2008 GU20	02/05/2016	21.49	0.45	0.67	1.26	NOISY
	2012 JR17	02/05/2016	19.72	0.81	0.41	0.83	X
467527	2007 LA15	02/05/2016	20.59	0.81	0.38	0.79	X/S
468004	2012 XD17	02/05/2016	20.95	0.66	0.30	0.72	X
	2013 KJ6	03/06/2016	20.17	0.73	0.46	0.57	S
467335	2002 JA9	03/06/2016	20.27	0.87	0.67	1.00	S

Object Name		Observational date	V	B-V	V-R	V-I	Taxonomy
	2016 JN17	03/06/2016	20.83	0.77	0.51	0.90	S
468468	2004 KH17	03/06/2016	19.28	0.78	0.54	0.65	S
469722	2005 LP40	03/06/2016	20.45	0.94	0.42	0.83	S
	2016 CF194	03/06/2016	19.63	0.72	0.64	1.00	S
	1999 VR6	03/06/2016	20.15	0.61	0.50	0.74	C
	2007 VT6	03/06/2016	19.90	0.73	0.31	0.46	C
	2016 BU13	03/06/2016	19.42	0.79	0.38	0.59	C
436771	2012 JG11	03/06/2016	20.43	0.88	0.43	0.68	S
	2016 LA9	02/07/2016	19.61	0.64	0.45	0.98	X
470594	2008 MN1	02/07/2016	19.29	0.38	0.25	0.72	NOISY
	2016 GN221	02/07/2016	19.23	0.88	0.40	0.76	S
469722	2005 LP40	02/07/2016	20.83	0.58	0.59	0.98	S
436771	2012 JG11	02/07/2016	20.39	0.84	0.47	0.84	S
468741	2010 VM1	02/07/2016	18.60	0.76	0.32	0.69	C
333578	2006 KM103	02/07/2016	19.74	0.82	0.47	0.65	V
468540	2006 MD12	02/07/2016	20.12	0.76	0.48	0.71	S
468452	2003 SD170	02/07/2016	18.86	0.74	0.33	0.63	C
	2016 LS9	02/07/2016	19.47	0.73	0.29	0.34	NOISY
457663	2009 DN1	02/07/2016	19.58	0.80	0.38	***	X
216523	2001 HY7	02/07/2016	18.97	0.58	0.43	0.52	NOISY
	2016 LY47	02/07/2016	19.90	***	0.50	0.72	S
	2014 KZ45	02/07/2016	19.58	0.90	0.75	1.13	S
470310	2007 LB15	30/07/2016	20.11	0.90	0.23	0.68	C/X
	2016 NW22	30/07/2016	20.20	***	0.37	0.68	C
	2001 UG18	30/07/2016	19.88	1.11	0.41	0.49	S
486001	2012 MR7	30/07/2016	20.67	***	0.21	0.82	NOISY
468684	2009 QY33	30/07/2016	21.77	0.83	0.58	1.60	NOISY
	2016 LZ10	30/07/2016	17.91	0.80	0.40	0.65	C
417167	2005 WH57	30/07/2016	20.74	1.09	0.28	0.64	C
	2016 NV	30/07/2016	20.01	1.03	0.50	1.79	S
474451	2003 SR15	02/09/2016	19.96	0.86	0.35	0.97	S
474706	2005 GC141	02/09/2016	21.33	0.79	0.73	1.23	NOISY
	2012 ES14	02/09/2016	19.64	0.69	***	0.91	D
474238	2001 RU17	02/09/2016	18.80	0.75	0.44	0.80	S

Object Name		Observational date	V	B-V	V-R	V-I	Taxonomy
474613	2004 TL19	02/09/2016	21.25	0.58	0.37	0.73	C
	2016 EL158	02/09/2016	20.13	0.63	0.55	0.92	S
	2009 VY25	02/09/2016	18.82	0.61	0.37	0.69	C
	2014 RC11	02/09/2016	20.30	0.86	0.52	0.88	S
	2016 AZ65	02/09/2016	21.81	***	0.57	1.92	NOISY
477719	2010 SG15	30/09/2016	20.90	***	0.51	***	NOISY
	2014 SD224	30/09/2016	21.58	0.66	0.81	0.81	S
	2016 GD135	30/09/2016	20.34	***	0.60	0.71	S
	2005 UE	30/09/2016	20.28	0.73	0.47	0.79	S/X
	2005 TF	30/09/2016	18.62	0.89	0.35	0.60	C
474163	1999 SO5	30/09/2016	18.78	0.91	0.30	0.58	C
414960	2011 CS4	30/09/2016	18.57	0.77	0.40	0.77	X
	2016 OJ1	30/09/2016	19.94	1.56	***	0.61	NOISY
420738	2012 TS	30/09/2016	20.00	0.68	0.39	***	C
	2005 CL	22/10/2016	20.93	0.98	0.49	0.67	S
	2002 UQ12	22/10/2016	19.49	0.58	0.40	0.65	C
467347	2003 GR	22/10/2016	20.08	0.68	0.48	***	X
	2013 FY13	22/10/2016	20.37	***	0.42	0.96	NOISY
	2004 TK10	22/10/2016	20.60	0.39	0.38	***	NOISY
	2015 BV92	22/10/2016	21.19	0.99	***	***	NOISY
	2015 BY310	27/02/2016	19.69	0.81	0.27	0.56	C
	2013 CL118	27/02/2016	20.45	0.64	0.38	0.69	C
	2016 UU80	27/02/2016	18.76	0.96	0.52	0.96	A
265482	2005 EE	27/02/2016	19.68	0.78	0.60	0.51	V
	2005 YV55	27/02/2016	20.62	0.79	0.43	0.55	C
	2003 EZ16	27/02/2016	20.40	0.63	0.44	0.63	C
	2014 DH23	27/02/2016	20.04	0.83	0.43	0.47	S
152671	1998 HL3	27/02/2016	19.69	0.97	0.37	0.86	S
317255	2002 DJ5	27/02/2016	18.79	0.79	0.33	0.58	C
484506	2008 ER7	27/02/2016	18.37	0.71	0.46	0.76	NOISY
	2009 EM1	27/02/2016	19.75	***	1.05	1.23	NOISY
164207	2004 GU9	27/02/2016	20.45	0.87	***	0.71	S

In order to investigate the relationship between taxonomic classification (and therefore surface composition) and dynamical properties, we analyzed the distribution of different taxa in our sample according to their orbital parameters: semi-major axis *a*, eccentricity *e*, inclination *i*, perihelion *q*, aphelion *Q* and *MOID* with our planet. The last in particular allows us to define the PHAs, which are objects with a MOID with the Earth < 0.05 au and an absolute magnitude H < 22. PHAs are therefore NEOs passing close to our planet and big enough to cause regional or even global damages (at least bigger than 140 m, assuming an average albedo of 0.14). Therefore, the characterization of their composition and their mitigation relevant quantities is crucial.

In Fig. 3-1 we show, as an example, the MOID with the Earth as a function of the orbital inclination of the observed NEOs. Our analysis shows that, in our sample, the majority of PHAs belongs to the S-complex, in agreement with the recent results of Perna et al. (2016 [RD3]). However, two C-complex objects (443880 and 465824) and two D-type bodies (430804 and 2006 HV5) objects show a very low MOID (< 0.03 au) and very high inclination (>10°). This is particularly interesting from a mitigation point of view, since NEOs with lower MOID tend to pass very close to our planet, and objects with higher inclination are not easily reached by a spacecraft in case of a possible mitigation missions (Holsapple 2004 [RD4]). Furthermore, the most advanced mitigation technique (the kinetic impactor) seems to be more challenging to be executed on a generally porous carbonaceous C-complex asteroid rather than a monolithic S-complex body (Perna et al. 2013 [RD5]). Therefore, the more porous C-complex and D-type objects in low MOID, high inclination orbits represent at the moment a greater risk in terms of mitigation, and should require in the next future a more detailed investigation.

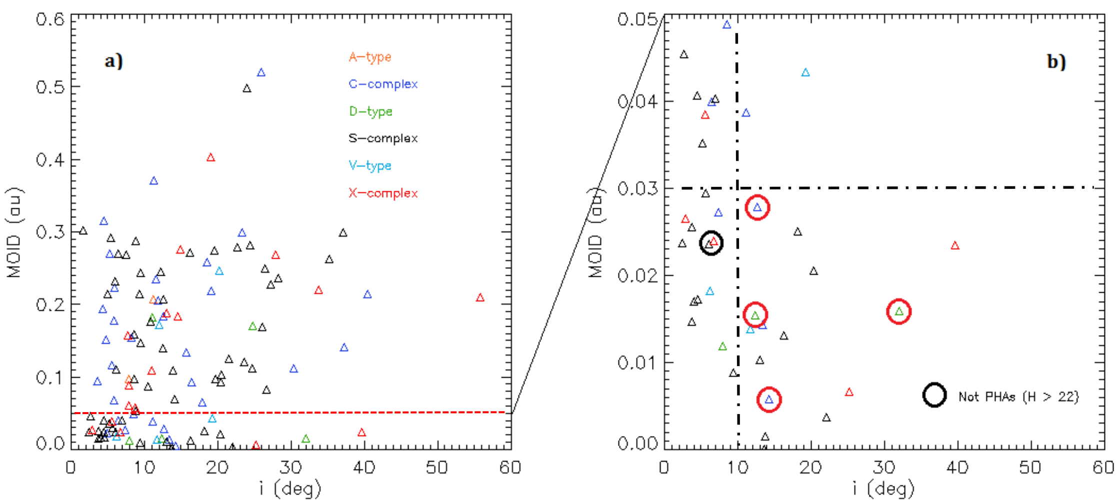

Figure 3-1 a) Inclination versus MOID reported for the whole sample and b) zoom on MOID < 0.05 au, which defines the PHA population. 4 NEOs circled in red represent at the moment the greatest threat in our sample, due to their porous nature, their high inclination and low MOID, and should require a detailed investigation. The two NEOs circled in black are not classified as PHA, because of their absolute magnitude, but are here reported for completeness.

2.1.2 Observations at LBT

We have obtained two separated runs of 2h each to observe NEOs at LBT in the B-V-R-I-g-r-z filters. 6 targets have been observed. Two of them (190166, 426071) are at the moment under further analysis. For 4 of them (267221, 313276, 426071, 2007VA85) data have been reduced and calibrated. Asteroid 2007 VA85 in particular was the subject of a dedicated analysis since, at its discovery, no clear evidence of coma and/or tail was detected in the images (Hicks et al. 2007 [RD6]) up to the last return in 2015-2016, when clearly comet-like activity was observed and the transient nature of the object was first hypothesized (Hicks & Tackeray, 2016 [RD7]), hence the new designation as 333P/2007 VA85 (PANSTARRS).

In order to identify the coma morphology and its surface colors we took 9 V and R short-term exposures (10.3 and 10.2 seconds each for the two filters, respectively). The images were prereduced (bias-subtracted and flat-fielded) by means of the LBT reduction pipeline, then an accurate background subtraction was performed using manually crafted procedures optimized for 333P/2007 VA85. Photometric calibration was performed using in-field standard stars of the APASS catalogue and proper conversion formulas, deriving an accurate Zero Point for each filter. Our analysis show that 333P/2007 VA85 shows two thin features within the antisolar tail-like structure and a broader structure extending from the nucleus towards the Sun (Fig. 3-2). Data analysis also pointed out that the coma show unusual blue colors, particularly when moving away from the nucleus.

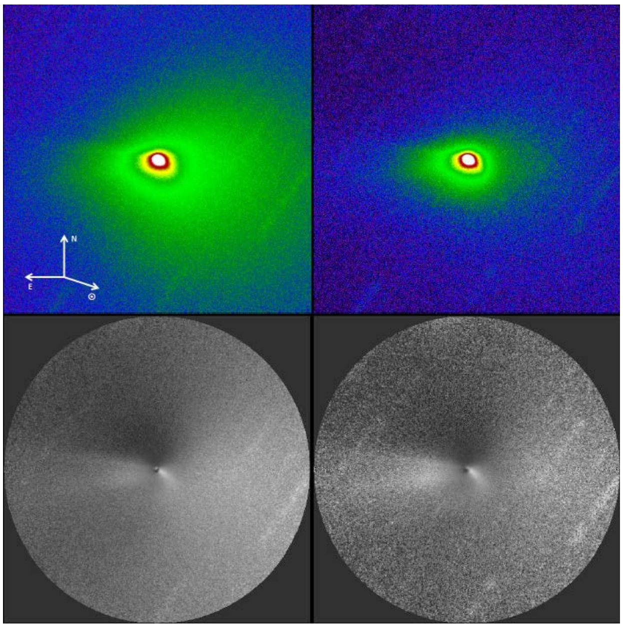

Figure 3-2 Top: V (left) and R (right) images of 333P/2007 VA85 obtained at LBT (inner part of the coma: the linear scale is 6.3 × 10^4 km). Bottom: corresponding processed images by means of the "azimuthal median" technique. At least two thin features within the antisolar tail-like structure and a broader structure extending from the optocentre (nucleus) towards the Sun are clearly visible.

2.1.3 Observations at Asiago

We used the 1m Asiago Schmidt telescope to characterize 37 NEOs in B-V-R-I filters. Results reported in Table 3-3 are ordered with decreasing V magnitude. Asteroids marked with an asterisk either do not have magnitudes measured in one or more filters, or their photometry presents large errors (either due to faint magnitudes or rotation to be confirmed). These asteroids would be re-observed in the next moths. Meanwhile, the whole sample is under analysis to obtain a preliminary taxonomic classification.

Table 3-3: Observational date and colour indexes for the whole sample of targets characterized at Asiago.

Object Name	Observational date	V	B-V	V-R	V-I
5143	14/11/2016	14.04	0.76	0.44	0.75
68950	29/10/2016	16.01	0.74	0.44	0.97
137170	27/04/2016	16.13	0.65	0.37	0.86
413002	17/01/2017	16.58	0.72	0.41	0.77
467963	10/11/2016	16.58	0.80	0.55	0.90

Object Name	Observational date	V	B-V	V-R	V-I
7341	30/10/2016	16.63	0.88	0.38	0.76
7350	25/04/2016	16.69	0.67	0.35	0.32
2005TF	30/10/2016	16.77	0.69	0.46	0.72
138847	29/04/2016	17.15	1.00	0.42	0.70
152931	17/01/2017	17.22	0.68	0.36	0.69
137032	29/10/2016	17.31	0.97	0.25	0.65
85990	19/01/2017	17.37	0.99	0.65	0.90
162269	29/10/2016	17.51	0.70	0.33	0.54
2006UM	29/10/2016	17.65	0.69	0.49	0.77
452389*	14/11/2016	17.69	***	0.11	0.94
326683	17/01/2017	17.76	0.93	0.47	0.81
1999VT	29/10/2016	17.82	0.75	0.36	0.66
2014EW24	20/01/2017	17.94	0.84	0.31	0.63
452389*	02/12/2016	18.06	0.74	0.61	1.43
203471	17/01/2017	18.10	0.45	0.12	0.33
465616*	29/04/2016	18.10	1.09	0.39	***
23187*	27/04/2016	18.11	0.83	0.49	***
414960	05/12/2016	18.12	1.08	-0.03	0.71
163243	29/04/2016	18.15	0.86	0.63	1.34
2013TV5*	30/10/2016	18.33	1.03	0.50	0.70
347813*	21/01/2017	18.36	0.73	0.52	1.01
2016UU80*	20/01/2017	18.36	0.47	0.51	0.72
363831*	30/11/2016	18.37	0.45	-0.09	0.31
2004TL19*	29/10/2016	18.54	0.99	0.48	0.90
2016QN11*	20/01/2017	18.75	1.04	***	0.89
254417	30/10/2016	18.80	0.76	0.38	0.66
265482*	15/02/2017	18.86	0.75	0.52	0.82
2016YT8	19/01/2017	19.32	0.60	0.36	0.54
357024*	02/12/2016	19.34	0.58	0.73	***
2012TQ78*	05/12/2016	19.37	0.58	0.48	1.23
479325*	14/02/2017	19.42	1.01	0.04	1.19
2005YS165*	15/02/2017	19.82	0.77	0.34	0.87

2.2 Phase curve characterization

The characterization of the phase curve of asteroids provides constraints on the absolute magnitude H of the body which, once the geometric albedo is known, relates the brightness of the asteroid to its size. Moreover, different surface compositions produce small changes in the shape of the phase curve, particularly in the so-called opposition surge effect, when the NEO reach 0° phase angle. The shape of the phase curve can therefore be used as a proxy to estimate the taxonomy of the asteroids (and the composition).

In order to characterize the very subtle differences in the phase curve characterization, we made use of an online tool (Penttilä et al. 2016 [RD8]), which fit the reduced data obtained for the target at different phase angles to derive a reliable estimation of their absolute magnitude H, their slope parameters (G1 and G2) and give a plausible taxonomic classification (see Tab. 3-5 and 3-7). The strength of our classification is assured by choosing the taxonomy with the smallest RMS (Penttilä et al. 2016 [RD8]), which is a general measure of the goodness of the fit.

2.2.1 Observations at Campo Imperatore

Since May 2016, we established a preferential access with the Italian Campo Imperatore observatory (L'Aquila) to perform phase curve characterization using the 1.3 square degrees FoV Schmidt telescope. With such a wide field instrument we performed infield calibration, allowing us to skip photometric correction due to different airmasses and to work even on non-photometric nights, a key feature for characterizing NEOs that are fading near the opposition surge.

After some technical issues with the instrumentation, observations started in August 2016. Our observations allowed to obtain phase curves for 29 objects (Tab. 3-4). For eight of them data has been already reduced and calibrated (40267, 480824, 2001 UG18, 2005 EC224, 2016 WU3, 2008 ER7, 2017 CR32, 2017 AC5). The remaining sample is at the moment under reduction and calibration. 8 NEOs were re-observed at OASI – Itacuruba in order to enlarge the statistical sampling of the data or extend the phase curve characterization to a broader range of phase angles. These objects are indicated in Tab. 3-4 and Tab. 3-5 with an asterisk.

Table 3-4: Observational date, phase angle range and comments for the phase curves obtained at Campo Imperatore.

Object	Observational date	Phase angle range	Comments
470510*	26/8-29/9/2016	0.7°-36.7°	*Data under reduction*
480824	27/9/2016 21/11/2016-1/1/2017	28.9° 1.9°-15.7°	Data reduced
370307	18/10/2016 11/3-22/4/2017	43.4° 3.8°-18.8°	*Data under reduction*
16816	15/11-7/12/2016	13.3°-25.5°	*Data under reduction*
2005 TF*	15/11-10/12/2016	17.9°-32.4°	*Data under reduction*
2001 UG18	15/11-17/12/2016	2.5°-19.1°	Data reduced
326683*	30/11/2016-1/1/2017	3.2°-39.0°	Data reduced
2016 UN36	30/11/2016-1/1/2017	1.0°-20.8°	*Data under reduction*
2016 WU3	30/11/2016-1/1/2017	4.8°-30.8°	Data reduced
253133	6-28/12/2016	1.1°-7.4°	*Data under reduction*
2016 WV	6/12/2016-1/1/2017	4.4°-16.4°	*Data under reduction*
10860	10/12/2016-1/1/2017	1.1°-9.7°	*Data under reduction*

Object	Observational date	Phase angle range	Comments
159608	10/12/2016-11/1/2017	2.9°-17.2°	*Data under reduction*
24525	10/12/2016-1/2/2017	3.9°-24.5°	*Data under reduction*
2014 YC	10/12/2016-1/2/2017	5.8°-30.8°	*Data under reduction*
2016 YF	23/12/2016-1/1/2017	1.2°-57.3°	*Data under reduction*
138846	23/12/2016-11/1/2017	4.5°-17.0°	*Data under reduction*
2014 AD17*	23/12/2016-11/1/2017	4.7°-17.9°	*Data under reduction*
2014 DH23	13/2-2/3/2017	1.7°-12.6°	*Data under reduction*
370702*	19/2-28/3/2017	1.9°-30.3°	Data reduced
40267*	19/2-28/3/2017	2.8°-26.6°	Data reduced
4055*	19/02-31/03/2017	2.0°-13.7°	*Data under reduction*
2017 AC5	20/02-9/4/2017	5.4°-26.4°	Data reduced
357621	21/2-3/3/2017	1.3°-5.1°	*Data under reduction*
484506*	21/2-31/3/2017	3.2°-22.8°	Data reduced
474451	16-29/3/2017	2.3°-13.6°	*Data under reduction*
2017 CR32	16-31/03/2017	2.0°-19.1°	Data reduced
2017 DC38	17-31/03/2017	1.2°-11.2°	*Data under reduction*
175189	16/3-22/4/2017	0.7°-29.4°	Data reduced

In Fig. 3-3 and Tab. 3-5 we reported as example seven phase curve analysis performed, a reliable estimation of their absolute magnitude H and a plausible taxonomic classification using the online tool developed by Penttilä et al. (2016 [RD8]), together with the RMS which indicates the robustness of the fit.

Table 3-5: Phase curve parameters (H, G1 and G2) derived using the online tool by Penttilä et al. (2016) for seven objects observed at Campo Imperatore.

Object	Observational date	H	G1	G2	taxonomy	RMS
2001 UG18	15/11-17/12/2016	20.62 ± 0.41	0.259	0.372	S/M	0.409
175189	16/3-22/4/2017	18.36 ± 0.44	0.834	0.049	P	0.463
484506	21/2-31/3/2017	20.02 ± 0.17	0.150	0.600	E	0.219
2016 WU3	30/11/2016-1/1/2017	20.25 ± 0.32	0.823	0,019	C	0.320
40267	19/2-28/3/2017	15.55 ± 0.70	0.962	0.016	D	0.717
480824	27/9/2016 21/11/2016-1/1/2017	16.60 ± 0.21	0.823	0.019	C	0.358
2017 CR32	16-31/3/2017	22.36 ± 0.62	0.961	0.016	D	0.610

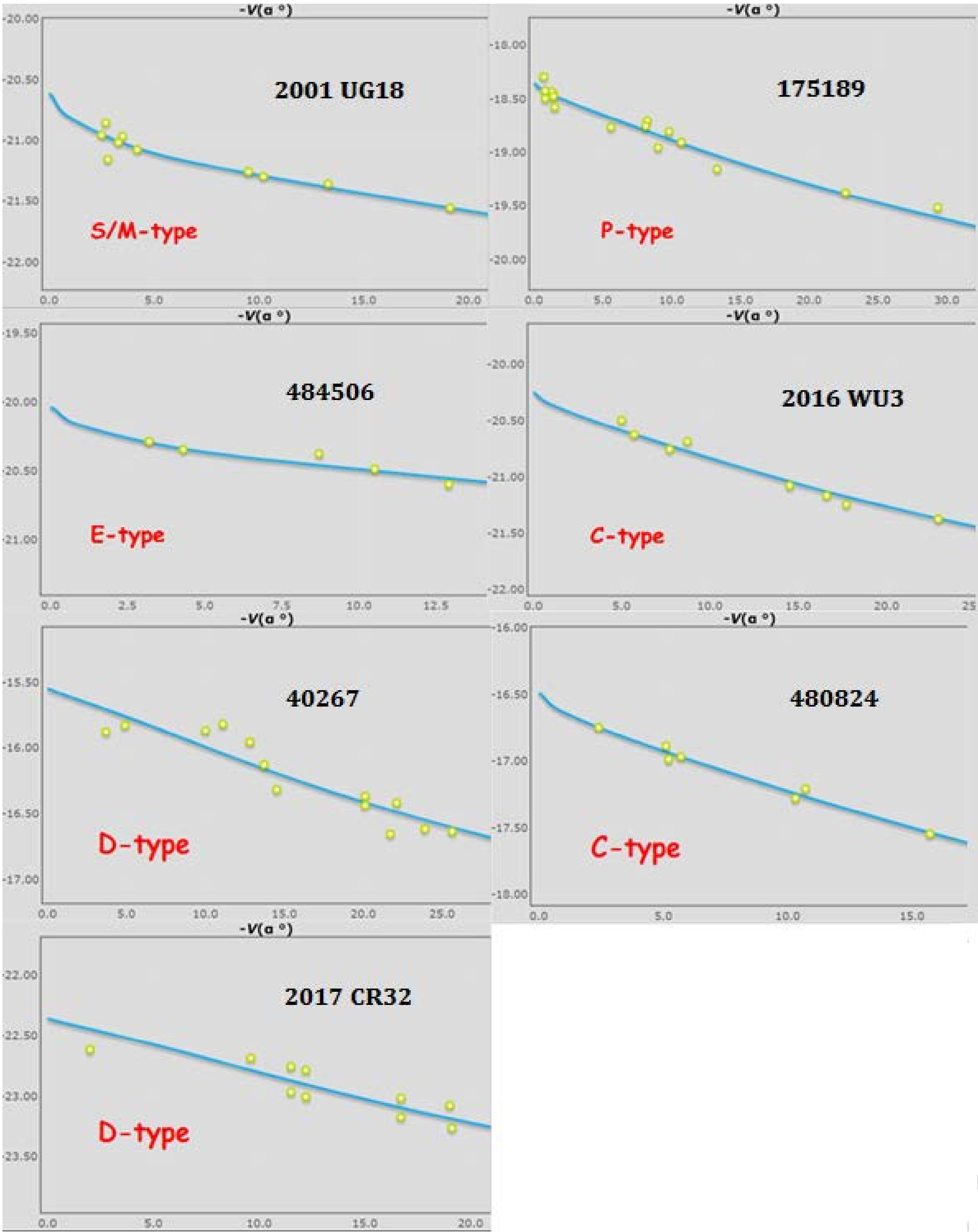

Figure 3-3: Phase curves analysed using the online tool derived by Penttilä et al. (2016) for seven objects observed at Campo Imperatore.

2.2.2 Observations at OASI

We established a collaboration with the Observatorio Nacional do Rio de Janeiro (D. Lazzaro) to use the Brazilian 1m-telescope in the OASI to obtain photometric observations of NEOs at different phase angles and perform phase curve characterization. Observations started in September 2015, although we had some technical issues with the dome and the CCD that have delayed the scheduled observations for several months. Furthermore, the winter weather in

Itacuruba is heavy rainy and we lost some nights of observations, which can be dramatic in the phase curve characterization of fading NEOs.

We managed to obtain phase curves for 29 objects (Tab. 3-6). For four of them (333889, 337118, 446833, 4055) data has been already reduced and calibrated (see Fig. 3-4). The remaining sample is at the moment under reduction and calibration.

Table 3-6: Observational date, phase angle range and comments for the phase functions obtained at OASI – Itacuruba.

Object	Observational date	Phase angle range	Comments
333889	9-18/09/2015	25°-4°	Data reduced
337118	9-18/09/2015	32°-11°	Data reduced
446833	9-18/09/2015	9°-27°	Data reduced
4055*	9-18/09/2015 19/02-05/03/2017	4°-16° 10°-2°	Data reduced *Data under reduction*
330825	5-10/06/2016 28/06-10/07/2016	6°-17°	*Data under reduction*
2016 BX14	5-10/06/2016 28/06-10/07/2016	30°-2°	*Data under reduction*
468448	28/06-10/07/2016 26/07-08/08/2016	25°-14°	*Data under reduction*
2016 NA1	26/07-08/08/2016	9°-22°	*Data under reduction*
2016 NX	26/07-08/08/2016	17°-24°	*Data under reduction*
470510*	26/07-08/08/2016 25/08-08/09/2016	22°-0.5°	*Data under reduction*
469634	25/08-08/09/2016 23/09-07/10/2016	29°-13°	*Data under reduction*
464797	25/08-08/09/2016	8°-25°	*Data under reduction*
480004	23/09-07/10/2016	27°-15°	*Data under reduction*
2016 RP33	23/09-07/10/2016	7.5°-23°	*Data under reduction*
474163	23/09-07/10/2016	24°-15°	*Data under reduction*
2005 TF*	23/09-07/10/2016 23-28/10/2016	14°-4°	*Data under reduction*
36236	21/11-6/12/2016	8°-13°	*Data under reduction*
326683*	21/11-6/12/2016	25°-4°	*Data under reduction*
2016 WJ1	21/11-6/12/2016	5°-25°	*Data under reduction*
3360	21/11-6/12/2016	12°-5°	*Data under reduction*
34613	21/01-4/02/2017	1°-9°	*Data under reduction*
2001 QE34	21/01-4/02/2017	5°-25°	*Data under reduction*
438955	21/01-4/02/2017	25°-5°	*Data under reduction*
2014 AD17*	21/01-4/02/2017	6°-16°	*Data under reduction*
2017 AF5	21/01-4/02/2017	16°-8.5°	*Data under reduction*
40267*	19/02-05/03/2017	2°-16°	*Data under reduction*
370702*	19/02-05/03/2017	1.5°-8°	*Data under reduction*

Object	Observational date	Phase angle range	Comments
484506*	19/02-05/03/2017	25°-3°	*Data under reduction*

In Tab. 3.7 and Fig. 3-4 we reported phase curves for the 4 NEOs characterized at OASI in September 2015, and the possible taxonomic class we found, together with the RMS which indicates the robustness of the fit.

Table 3-7: Phase curve parameters (H, G1 and G2) derived using the online tool by Penttilä et al. (2016) for four objects characterized at OASI – Itacuruba.

Object	Observational date	H	G1	G2	taxonomy	RMS
4055	9-18/09/2015	14.43 ± 0.24	0.810	0.015	V	0.752
333889	9-18/09/2015	17.64 ± 0.38	0.259	0.372	S/M	0.644
337118	9-18/09/2015	17.77 ± 0.47	0.151	0.600	E	1.149
446833	9-18/09/2015	20.40 ± 0.35	0.258	0.372	S/M	0.169

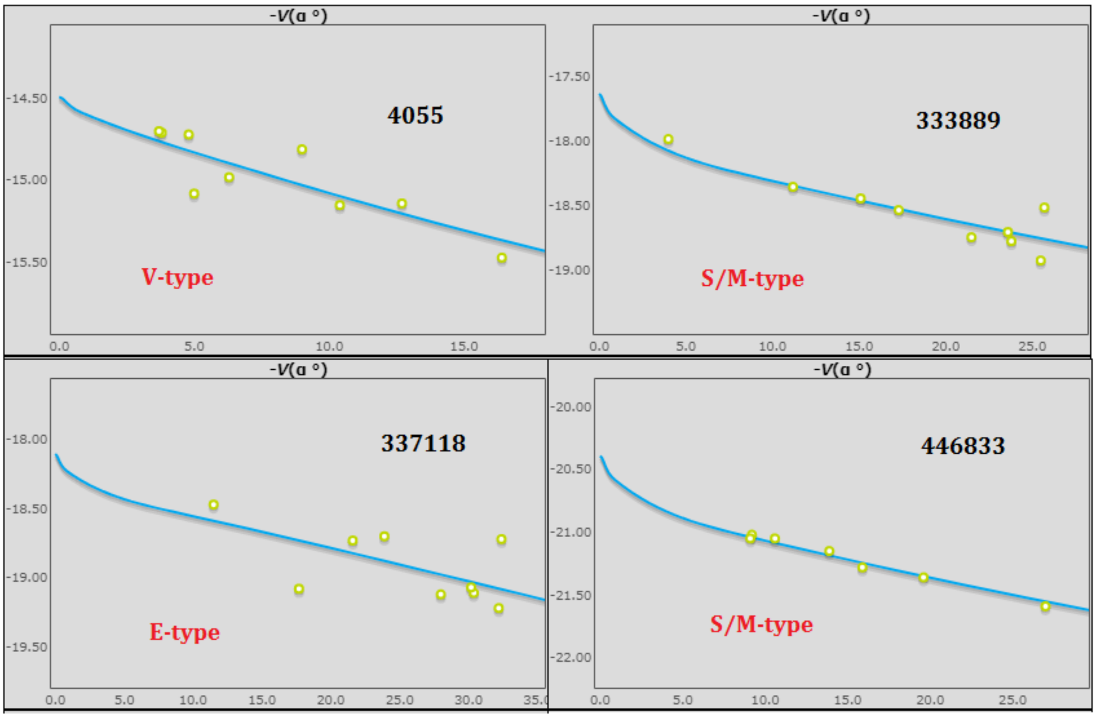

Figure 3-4 Phase curves analysed using the online tool derived by Penttilä et al. (2016) for four targets observed at OASI – Itacuruba telescope in September 2015: (4055) and (333889) on top and (337118) and (446833) on bottom.

3 Summary

We report hereafter a brief summary of our main results in the framework of the task 10.2.1 of the NEOShield-2 project.

- As of today, we have obtained from our facilities (TNG, LBT and Asiago) B-V-R-I (and in some cases also g-r-z) photometric measurements for a total sample of 231 previously uncharacterized NEOs, although this is at the moment a lower-limit estimation, since two more runs are available in the framework of the LTP. Indeed, we managed a 2-year LTP at TNG dedicated to the physical characterization of the small NEO population (September 2015 – September 2017). This study is particular important not only because the small NEO population has at the moment sparse data in literature, but it is also the one with the highest likelihood of having a potential impact with our planet in the next centuries. We have obtained a preliminary taxonomic classification for most of the objects in our sample and we have analysed the distribution of different taxa according to their orbital parameters. Our results show that porous C-complex bodies with a low MOID with our planet and on high inclination orbits represent at the moment a greater risk in terms of mitigation, and should require in the future a detailed investigation.
  These data and the subsequent analysis will be featured in two articles, with the one on results of the first year of the LTP at the moment under redaction (Ieva et al., in preparation).

- We have characterized the coma morphology and the surface colours of the object 333P/2007 VA85. At its discovery, this body show no evidence of cometary nature, up until its last return in 2015-2016, when clearly comet-like activity was observed and the transient nature of the object was first hypothesized. Our analysis show that 333P/2007 VA85 not only has two features in the antisolar direction, but also a broader structure extending from the nucleus toward the Sun. The coma shows also unusual blue colors when moving away from the nucleus.
  These results will soon be published in an article currently in preparation (Dotto et al., in prep.).

- We have obtained phase curve characterization for a total of 49 NEOs. 8 targets were observed from both the facilities of Campo Imperatore and OASI – Itacuruba in order to enlarge the statistical sampling of the data or extend the phase curve characterization to a broader range of phase angles. We made use of an online tool to obtain a reliable estimation of the taxonomic class and their slope parameters. At the moment, we have obtained reliable phase functions characterization for 11 objects. The remaining data is at the moment under reduction and calibration.
  Phase curve analysis will be featured in an at least one article at the moment under redaction (Ieva et al., in prep.).

All the data obtained within this Task will be soon entered into the NEOShield-2 physical properties open data repository and will be eventually available via the ESA - NEOCC.